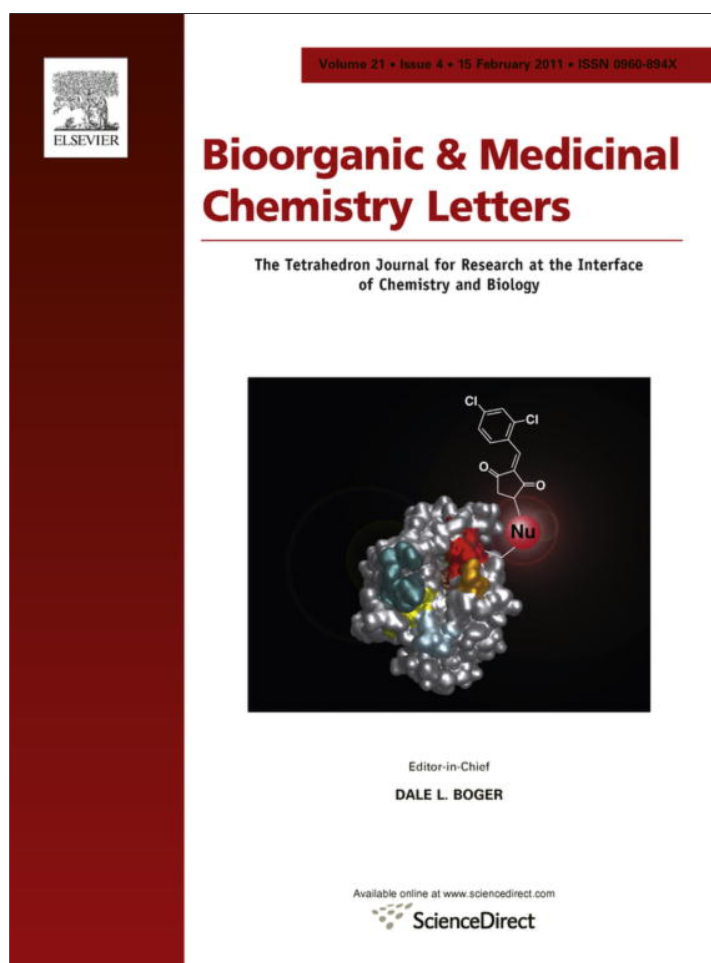


Provided for non-commercial research and education use.  
Not for reproduction, distribution or commercial use.



This article appeared in a journal published by Elsevier. The attached copy is furnished to the author for internal non-commercial research and education use, including for instruction at the authors institution and sharing with colleagues.

Other uses, including reproduction and distribution, or selling or licensing copies, or posting to personal, institutional or third party websites are prohibited.

In most cases authors are permitted to post their version of the article (e.g. in Word or Tex form) to their personal website or institutional repository. Authors requiring further information regarding Elsevier's archiving and manuscript policies are encouraged to visit:

<http://www.elsevier.com/copyright>



Contents lists available at ScienceDirect

# Bioorganic & Medicinal Chemistry Letters

journal homepage: [www.elsevier.com/locate/bmcl](http://www.elsevier.com/locate/bmcl)

## Identification of small molecular inhibitors for Ero1p by structure-based virtual screening

Yanyan Chu<sup>a</sup>, Xianjun Chen<sup>a,b</sup>, Yi Yang<sup>a,b,\*</sup>, Yun Tang<sup>a,c,\*</sup><sup>a</sup> Department of Pharmaceutical Sciences, School of Pharmacy, East China University of Science and Technology, Shanghai 200237, China<sup>b</sup> State Key Laboratory of Bioreactor Engineering, East China University of Science and Technology, Shanghai 200237, China<sup>c</sup> State Key Laboratory of Drug Research, Shanghai Institute of Materia Medica, Chinese Academy of Sciences, Shanghai 201203, China

### ARTICLE INFO

#### Article history:

Received 20 October 2010

Revised 13 December 2010

Accepted 24 December 2010

Available online 1 January 2011

#### Keywords:

Virtual screening

Ero1p

Disulfide bond

Protein disorder

Oxidoreductase

### ABSTRACT

Ero1p, using molecular oxygen as its preferred terminal electron acceptor, promotes disulfide bond formation by interaction with protein disulfide isomerase. Dysfunction of Ero1p leads to strong activation of the unfolded protein response and marked loss of cell viability. However, modest attenuation of Ero1p improves the fitness of yeast challenged with high levels of protein misfolding in their endoplasmic reticulum stress. Partial inhibition of Ero1p is hence of great significance. In the present paper, a docking-based virtual screening method was performed to identify inhibitors of Ero1p and 12 hits were successfully obtained from 81 purchased compounds with micromolar inhibition against Ero1p. Particularly, six of the hits demonstrated remarkable potency with  $IC_{50} < 30 \mu M$  and held the prospect of becoming lead compounds. Then the interaction modes were analyzed for further lead optimization.

© 2010 Elsevier Ltd. All rights reserved.

Many extracellular proteins require the formation of one or more disulfide bonds to achieve their correct tertiary structure. Protein folding disorder will result in lots of diseases such as diabetes, arthritis, cancer, cardiovascular disease, and neurodegenerative diseases.<sup>1</sup> Endoplasmic reticulum oxidoreductin-1 protein (Ero1p),<sup>2,3</sup> a membrane-associated flavoprotein,<sup>4</sup> promotes disulfide bond formation in the endoplasmic reticulum (ER) by selectively oxidizing the soluble oxidoreductase–protein disulfide isomerase (PDI), which in turn can directly oxidize secretory proteins.

Ero1p is an essential enzyme in yeast. It requires flavin adenine dinucleotide (FAD) as a cofactor to support the oxidation of disulfide-containing substrates. The activity of Ero1p is modulated by luminal FAD levels.<sup>5–7</sup> However, by now it is still unknown how FAD is transported into the ER. Ero1p is the source of disulfide bonds,<sup>3</sup> because molecular oxygen is used as its preferred terminal electron acceptor. Crystal structure of Ero1p suggests that the protein contains five disulfide bonds. The core of Ero1p is highly helical with loops covering the surface of the protein. Two redox-active disulfide bonds are essential for Ero1p oxidase activity: Cys352–Cys355 and the shuttle cysteines Cys100–Cys105. The activity of Ero1p can also be modulated through the redox state of two non-essential ‘regulatory’ cysteine pairs (Cys90–Cys349

and Cys150–Cys295) by controlling the range of motion for the shuttle-cysteine-containing loop region.<sup>8,9</sup> Genetic and structural data indicate that a disulfide bond is transferred from Cys100–Cys105 directly to PDI, whereas the Cys352–Cys355 disulfide bond is used to reoxidize the reduced Cys100–Cys105 pair through an internal thiol-transfer reaction.<sup>4</sup> The Cys352–Cys355 motif abuts the cofactor FAD. So then Cys352–Cys355 is reoxidized by transferring their electrons to FAD and further to molecular oxygen. Considerable efforts have been devoted towards Ero1p and the process of disulfide formation, which broadened our understanding to the redox pathways.

It was reported that the dysfunction of Ero1p lead to a rapid decline in oxidative protein folding, strong activation of the unfolded protein response, and marked loss of viability.<sup>2,10,11</sup> In 2004, Haynes group found that modest attenuation of Ero1p activity could improve the fitness of yeast challenged with high levels of protein misfolding in their ER.<sup>12</sup> Moreover, Ero1-L $\alpha$ , the closest known homolog with Ero1p in human, was strongly upregulated by hypoxia and independent of hypoglycemia, two known accompaniments of tumors.<sup>13</sup> Upregulation of Ero1-L $\alpha$  by hypoxia was demonstrated in a variety of tumor cell lines, and it was the only gene induced by hypoxia.<sup>13</sup> So Ero1-L $\alpha$  expression in tumor cells might be a potential therapeutic target for future cancer therapies.<sup>13</sup> Otherwise, lowered levels of Ero1 activity can protect against severe ER stress in worms, yeast and mammalian cells.<sup>11,12,14,15</sup> It suggests potential benefits for partial inhibition of Ero1. Moreover, an inhibitor of Ero1 with selectively reverse thiol reactivity, EN460, was found by a high-throughput in vitro assay with  $IC_{50}$  value at 1.9  $\mu M$  (Fig. 1).<sup>11</sup> And

\* Corresponding authors. Tel.: +86 21 6425 1052; fax: +86 21 6425 3651.

E-mail addresses: [yiyang@ecust.edu.cn](mailto:yiyang@ecust.edu.cn) (Y. Yang), [ytang234@ecust.edu.cn](mailto:ytang234@ecust.edu.cn) (Y. Tang).

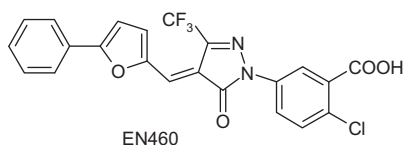


**Figure 1.** Structure of the known small molecular inhibitor of Ero1.<sup>11</sup>

the action mechanism of EN460 suggested that reductive inactivation of Ero1 by EN460 lead to weakened binding of FAD. EN460 labeling of Ero1 promoted loss of FAD from the holoenzyme.<sup>11</sup> In our previous studies on Ero1-L $\alpha$ , we had already investigated the property of FAD binding pocket and compared the differences of FAD binding with Ero1-L $\alpha$  and Ero1p.<sup>16</sup>

In the present work, to find potential inhibitors of Ero1p, we turned to docking-based virtual screening, which can evaluate millions of molecules rapidly and inexpensively. All the programs used were from Schrödinger suite package. In the beginning, the crystal structure of yeast Ero1p complexed with FAD was retrieved from the Protein Data Bank (<http://www.rcsb.org/pdb/>), PDB code: 1RP4.<sup>3</sup> The missing side chains of residues were added by Prime (version 2.0).<sup>17</sup> FAD and crystal water molecules around 5 Å of FAD were retained. Other crystal waters and nonstandard amino acids were removed from the crystal structure of the complex. All MSE residues were mutated back to MET. Then the complex was prepared and minimized by Protein Preparation Wizard. Thanks to the essential roles of FAD playing in the activity of Ero1p, we focused mainly on the FAD binding pocket to search for a lead which would compete with FAD to bind with the enzyme. In the next step, the target pocket was defined by a grid with outer box dimensions of 14 Å centered with the FAD cofactor. The docking program Glide (version 5.0)<sup>18</sup> was performed in standard precision (SP) mode to dock a library of 197,116 compounds from SPECS database (<http://www.specs.net/>) flexibly. Before carrying out Glide screening, all compounds in the database were treated with LigPrep (version 2.2)<sup>19</sup> to generate lowest energy conformations. The Schrödinger's proprietary GlideScore was used to roughly approximate the binding affinity of each molecule with Ero1p, and hence to rank the virtual hits. The docking results yielded a chemically diverse set of compounds. We inspected the ranked top 1000 compounds visually. The compounds with interaction modes and conformations similar to FAD, especially in the position isoalloxazine ring occupied, were retained. Finally, 81 compounds were selected as hits and purchased from the SPECS Company.

A continuous fluorescence assay was used to monitor the activity of each compound against yeast Ero1p. At the beginning, each of the compounds was dissolved with DMSO (Dimethyl Sulfoxide) and diluted into different concentrations (5 mg/ml, 1 mg/ml, 500  $\mu$ g/ml, 250  $\mu$ g/ml, 100  $\mu$ g/ml, 50  $\mu$ g/ml) to obtain compound solutions. Then, 27  $\mu$ L of Ero1p enzyme was mixed with 3  $\mu$ L compound solution, and 30  $\mu$ L of the mixture was obtained. Afterward, we removed a 10  $\mu$ L aliquot of the mixture to the ultraviolet non-absorbable 384 well plate, then added the reaction solution that contained 5  $\mu$ L HVA (20 mM), 5  $\mu$ L HRP (28  $\mu$ M), 2  $\mu$ L TCEP (200 mM, pH 7.0) and 58  $\mu$ L PBS (containing 5 mM EDTA), followed by measuring the fluorescence dynamics at  $\lambda_{\text{ex}}360/40$ ,  $\lambda_{\text{em}}485/40$ . At last, IC<sub>50</sub> value was determined by plotting and fitting the inhibition curve using Sigma Plot. The IC<sub>50</sub> was indicated in the curve where the remained relative enzyme activity is 50%.

The results from biological tests showed that 12 out of the 81 purchased compounds displayed potent inhibition to Ero1p with IC<sub>50</sub> values below or around 100  $\mu$ M, corresponding to a hit rate of 14.8%. All the hits had docking scores lower than -9 in virtual screening. The results demonstrated that docking-based virtual screening with Glide is a viable strategy for inhibitor identification

against Ero1p. The structure and IC<sub>50</sub> value of each compound were shown in Figure 2. Among the 12 hits, compounds **1**, **3**, **7**, **9–11** showed significantly potent activities to Ero1p with IC<sub>50</sub> values below 30  $\mu$ M.

Comparing the structures of the hits and the known inhibitor EN460, we found that all the compounds contained elements of abundant ring structures which probably serve to displace FAD from Ero1p.<sup>11</sup> And 9 of the 12 hits, **1–4**, **6** and **9–12** contain the enone functional group, which is a potent Michael acceptor for a range of thiols including DTT and glutathione and required by EN460 for inhibition.<sup>11</sup> The common functionality probably indicates the similar action mechanism that the hits might displace bound FAD from the enzyme's active site and react with cysteine residues reversibly. Among these, compound **3** was the most similar compound to EN460. Compounds **5**, **7**, and **8** do not have the enone group. In the other aspect, compounds **1–4** and **6** share a common structural feature, a five-membered heterocyclic ketone in the equivalent position of the structures. Compounds **9–12** contain a common 3-benzyl-barbituric acid group, and the benzyl groups were substituted in the *para* position.

Docking studies on the hits and the known inhibitor EN460 were performed to reveal the detailed binding modes of the compounds with Ero1p. Even though the structures are diverse, careful analysis of the complexes revealed similar interaction modes of these compounds including EN460 in the binding pocket. Owing to the structural similarity, the reported EN460 and compounds **1** and **3** adopted the similar conformations and binding modes in the pocket (Fig. 3), while compound **2** orientated inversely (Fig. 3E). The aromatic moieties of the four compounds interact tightly with residues W200 and H231 by aromatic ring stacking, and with Y191 in the edge-to-face  $\pi$ - $\pi$  interaction mode. And the same interactions were also found in other hit compounds. Besides, there were four crystal waters, which played essential roles in the hydrogen bonded network. Especially, the water bridge formed between Y191 and the ligand was found in almost all the compounds. The O of the enone functional group of all compounds formed stable hydrogen bond with W200. The phenomenon sufficiently proved that our simulation was rational and FAD binding pocket is a prospective pocket for the inhibitor design. Meanwhile, differences were existed. Compared with compound **3**, EN460 formed more strict face-to-face  $\pi$ - $\pi$  interaction with W200, and H-bond with N<sup>6</sup> of H231 by the additional carboxyl group. The strong binding made EN460 possess even lower IC<sub>50</sub> value. Comparing the four compounds, we can see that hydrophobic interaction in the pocket around C355 is necessary, and thus non-polar group substitution in the aromatic ring around C355 would be favorable for the binding, because compounds **1** and **3** had expected inhibitory activities (Figs. 3D and B). However, polar group substitution in the aromatic ring might be not favored for binding in the active site, which made compound **2** binding inverted (Fig. 3E). Meanwhile, electrophilic group -Cl interacted with  $\pi$ -electron of W200, which might be the reason that compound **2** rotated the aromatic ring and possessed higher IC<sub>50</sub> value than compounds **1** and **3**.

Compounds **10**, **11**, and **12**, containing 3-benzyl-barbituric acid, were derived from compound **9**. And the extended chain did not change their inhibitory activities a lot, even though better aromatic ring stacking was formed (Figs. 3C and F). Thanks to Ar-OH forms stronger electrostatic interaction than the ether group, compound **9** was even more efficient than compound **11**. Compound **9** may potentially serve as a new scaffold for lead optimization. The  $\pi$ - $\pi$  interaction was highly desired for significant Ero1p affinity. The combination of the  $\pi$ - $\pi$  interaction and the high frequency of the enone group indicated that the hits might inhibit the enzyme either by displacement of FAD from the enzyme, or reaction with the Cys residue. Meanwhile, residues E186, R187, and R260

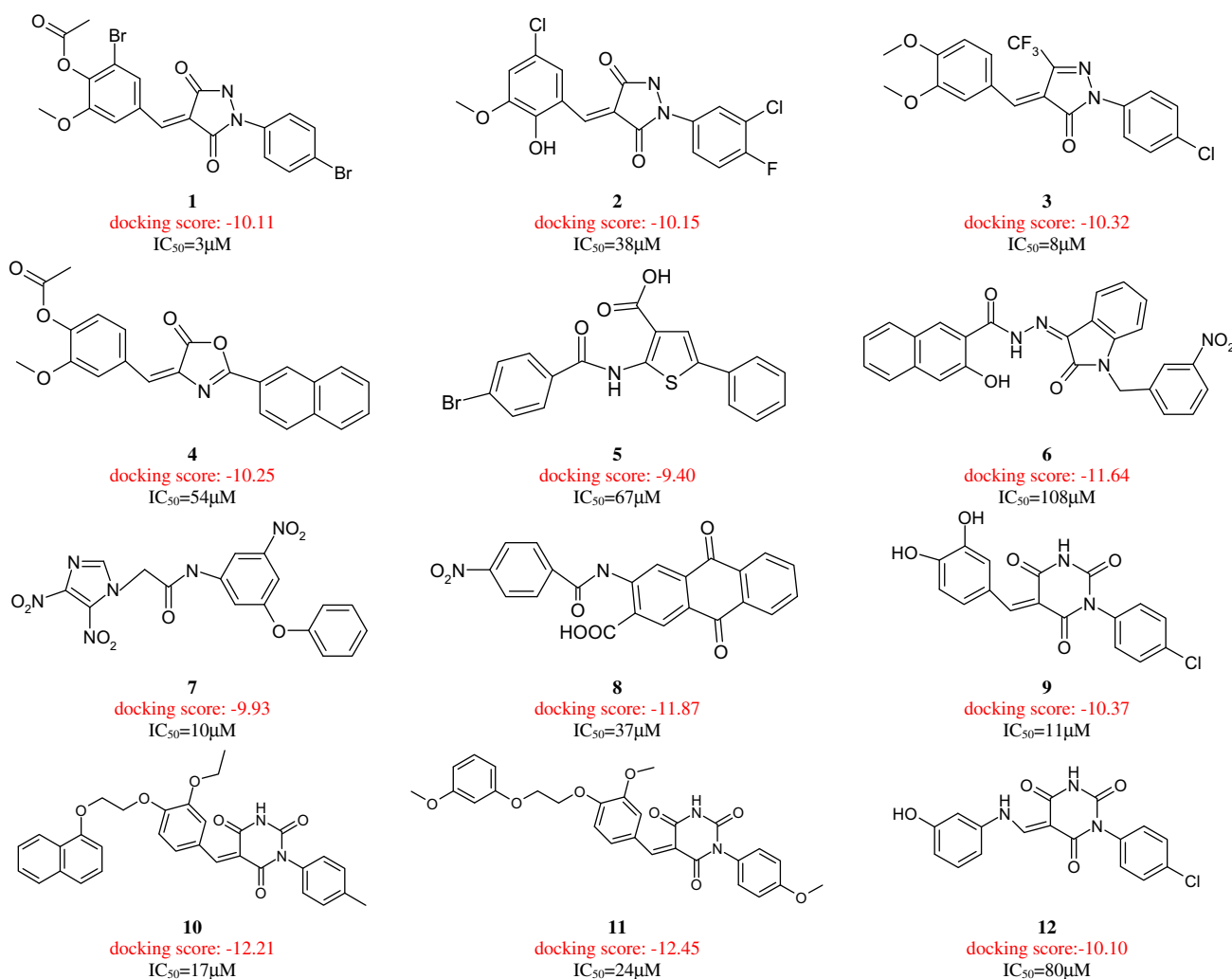


Figure 2. Structures, docking scores and inhibitory activities of the identified compounds.

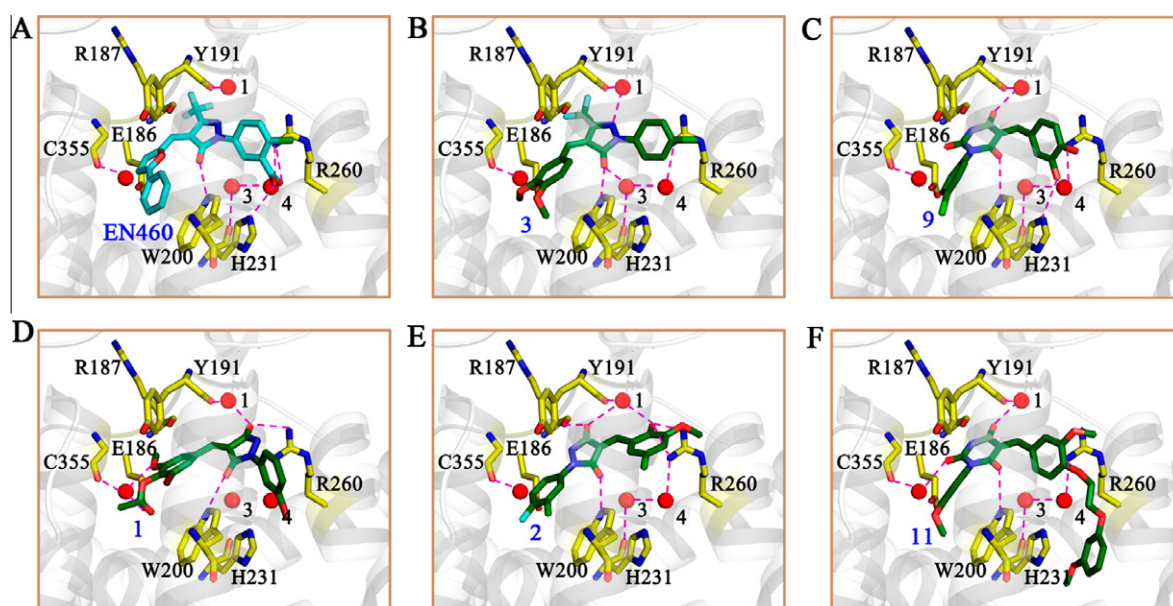
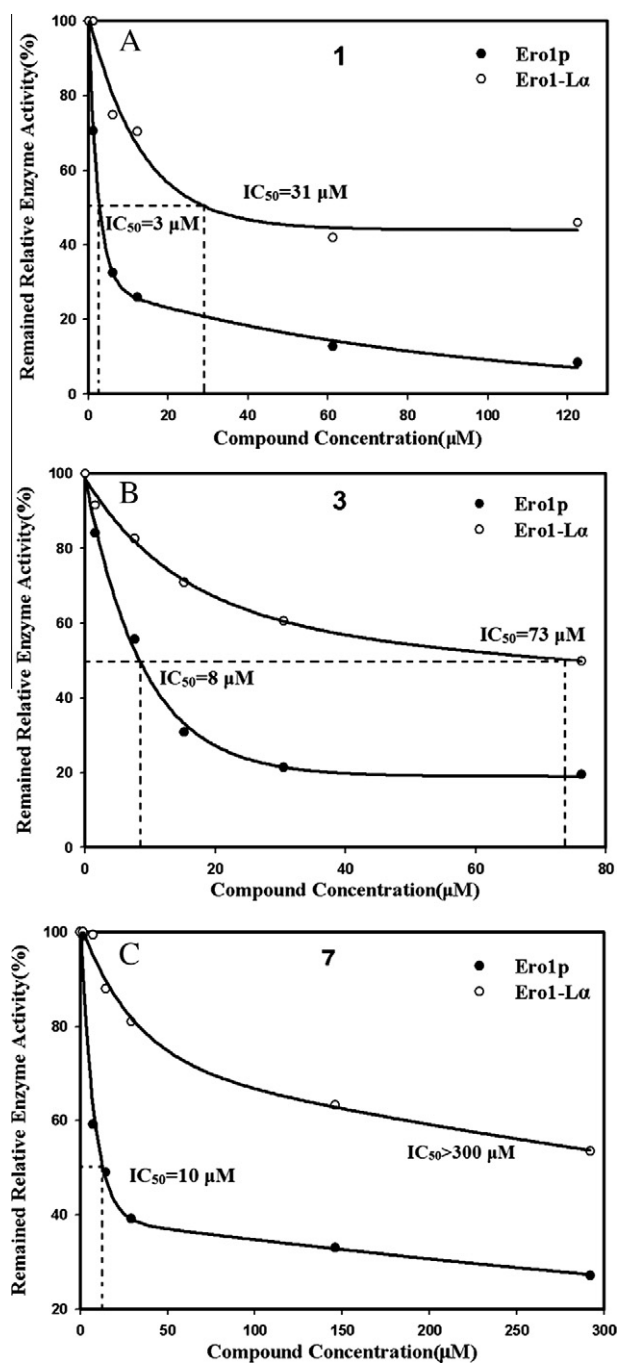


Figure 3. Close view of binding modes of compounds EN460 (A), 3 (B), 9 (C), 1 (D), 2 (E), and 11 (F) in the binding pocket of Ero1p (PDB code: 1RP4<sup>3</sup>). The Ero1p protein is shown in cartoon in light gray and hits are highlighted in green carbon. Hydrogen bonds are represented by violet dash lines. Important residues are labeled and represented by yellow carbon. The red spheres indicate crystal waters, which are important for the hydrogen bonded network.



**Figure 4.** Ero1p (solid core) and Ero1-L $\alpha$  (hollow) inhibitory activities for compounds **1** (A), **3** (B) and **7** (C). IC<sub>50</sub> values were marked.

were also important by the hydrogen bond network. Interestingly, we also noted that most of the compounds formed water bridges with C355, which probably inactivated the enzyme directly. Comparing the binding modes of different classes of the compounds,

we can conclude that lipophilic interaction was the most important, among which, residues Y191, W200 and H231 played indispensable roles for the hit compounds binding.

At the same time, we also tested the inhibitory activities of the compounds against human Ero1-L $\alpha$ . All the 12 hit compounds had inhibitory effects on the enzyme activity of Ero1-L $\alpha$ . Compounds **1**, **3** and **7** selectively inhibit Ero1p than Ero1-L $\alpha$ , the inhibition curves and corresponding IC<sub>50</sub> values were shown in Figure 4. Compounds **1** and **3** had about 10-fold inhibitory activities on Ero1p, compared with Ero1-L $\alpha$ . The IC<sub>50</sub> values of compound **1** were 3  $\mu$ M and 31  $\mu$ M for Ero1p and Ero1-L $\alpha$ , respectively. And the corresponding values for compound **3** were 8  $\mu$ M and 73  $\mu$ M. Among the three compounds, compound **7** showed the best inhibitory selectivity, with IC<sub>50</sub> values of 10  $\mu$ M and >300  $\mu$ M for Ero1p and Ero1-L $\alpha$ , respectively.

In summary, we have conducted a docking-based virtual screening on Ero1p successfully. Six hit compounds with excellent potency were discovered. Three compounds showed some selectivities for Ero1p and Ero1-L $\alpha$ . Molecular modeling studies on selected compounds were also presented to investigate the binding modes of the compounds with Ero1p. The information from careful analysis of the binding complexes would be useful for inhibitor design towards Ero1p. Meanwhile, this discovery validated docking-based virtual screening as a viable strategy for hit identification against Ero1p.

#### Acknowledgments

This work was supported by the Program for New Century Excellent Talents in University (Grant No. NCET-08-0774), the 111 Project (Grant No. B07023), the National S&T Major Project of China (Grant No. 2009ZX09501-001), Fok Ying Tung Education Foundation (Grant No. 111022), NSFC (Grant No. 90713026), and the State Key Laboratory of Drug Research.

#### References and notes

1. Metallo, S. J. *Curr. Opin. Chem. Biol.* **2010**, *14*, 481.
2. Pollard, M. G.; Travers, K. J.; Weissman, J. S. *Mol. Cell* **1998**, *1*, 171.
3. Gross, E.; Kastner, D. B.; Kaiser, C. A.; Fass, D. *Cell* **2004**, *117*, 601.
4. Sevier, C. S.; Kaiser, C. A. *Mol. Biol. Cell* **2006**, *17*, 2256.
5. Tu, B. P.; Weissman, J. S. *Mol. Cell* **2002**, *10*, 983.
6. Kettner, K.; Blomberg, A.; Rodel, G. *Yeast* **2004**, *21*, 1035.
7. Tu, B. P.; Ho-Schleyer, S. C.; Travers, K. J.; Weissman, J. S. *Science* **2000**, *290*, 1571.
8. Wang, L.; Li, S. J.; Sidhu, A.; Zhu, L.; Liang, Y.; Freedman, R. B.; Wang, C. C. *J. Biol. Chem.* **2009**, *284*, 199.
9. Sevier, C. S.; Kaiser, C. A. *Biochim. Biophys. Acta* **2008**, *1783*, 549.
10. Frand, A. R.; Kaiser, C. A. *Mol. Cell* **1999**, *4*, 469.
11. Blais, J. D.; Chin, K. T.; Zito, E.; Zhang, Y.; Heldman, N.; Harding, H. P.; Fass, D.; Thorpe, C.; Ron, D. *J. Biol. Chem.* **2010**, *285*, 20993.
12. Haynes, C. M.; Titus, E. A.; Cooper, A. A. *Mol. Cell* **2004**, *15*, 767.
13. May, D.; Itin, A.; Gal, O.; Kalinski, H.; Feinstein, E.; Keshet, E. *Oncogene* **2005**, *24*, 1011.
14. Marciniak, S. J.; Yun, C. Y.; Oyadomari, S.; Novoa, I.; Zhang, Y.; Jungreis, R.; Nagata, K.; Harding, H. P.; Ron, D. *Genes Dev.* **2004**, *18*, 3066.
15. Zito, E.; Chin, K. T.; Blais, J.; Harding, H. P.; Ron, D. *J. Cell Biol.* **2010**, *188*, 821.
16. Chu, Y.; Yang, C.; Chen, X.; Zheng, W.; Yang, Y.; Tang, Y. *Biochem. Biophys. Res. Commun.* **2009**, *389*, 645.
17. *Prime*, v., Schrödinger; LLC: New York, NY, 2008.
18. *Glide*, v., Schrödinger; LLC: New York, NY, 2008.
19. *LigPrep*, v., Schrödinger; LLC: New York, NY, 2005.